EFDA–JET–CP(12)01/09

G. Arnoux, S. Devaux, D. Alves, I. Balboa, C. Balorin, N. Balshaw, M. Beldishevski, P. Carvalho, M. Clever, S. Cramp, J.-L. de Pablos, E. de la Cal, D. Falie, R. Felton, P. Garcia-Sanchez, V. Gervaise, A. Goodyear, A. Horton, S. Jachmich, A. Huber, M. Jouve, D. Kinna, U. Kruezi, A. Manzanares, V. Martin, P. McCullen, V. Moncada, K. Obrejan, K. Patel, P. J. Lomas, A. Neto, F. Rimini, C. Ruset, B. Schweer, G. Sergienko, A. Soleto, M. Stamp, A. Stephen, P.D. Thomas, D.F. Valcárcel, J. Williams, J. Wilson, K.-D. Zastrow and JET EFDA contributors

# A Protection System for the JET ITER-Like Wall Based on Imaging Diagnostics

# A Protection System for the JET ITER-Like Wall Based on Imaging Diagnostics

G. Arnoux[1], S. Devaux[5], D. Alves[2], I. Balboa[1], C. Balorin[3], N. Balshaw[1], M. Beldishevski[1], P. Carvalho[2], M. Clever[4], S. Cramp[1], J.-L. de Pablos[6], E. de la Cal[6], D. Falie[7], P. Garcia-Sanchez[6], R. Felton[1], V. Gervaise[3], A. Goodyear[1], A. Horton[1], S. Jachmich[8], A. Huber[4], M. Jouve[3], D. Kinna[1], U. Kruezi[4], A. Manzanares[6], V. Martin[3], P. McCullen[1], V. Moncada[3], K. Obrejan[1], K. Patel[1], P. J. Lomas[1], A. Neto[2], F. Rimini[1], C. Ruset[7], B. Schweer[4], G. Sergienko[4], A. Soleto[6], M. Stamp[1], A. Stephen[1], P.D. Thomas[1], D.F. Valcárcel[2], J. Williams[1], J. Wilson[1], K.-D. Zastrow[1] and JET EFDA contributors*

***JET-EFDA, Culham Science Centre, OX14 3DB, Abingdon, UK***

*[1]EURATOM-CCFE Fusion Association, Culham Science Centre, OX14 3DB, Abingdon, OXON, UK*
*[2]Associação EURATOM/IST, Instituto de Plasmas e Fusão Nuclear, Instituto Superior Técnico, Universidade Técnica de Lisboa, P-1049-001, Lisboa, Portugal*
*[3]Association EURATOM-CEA, CEA/DSM/IRFM, Cadarache 13108 Saint Paul Lez Durance, France*
*[4]Forschungszentrum Jülich, Institute of Energy and Climate Research - Plasma Physics, EURATOM Association, D-52425, Jülich, Germany*
*[5]Max-Planck-Institut für Plasmaphysik, EURATOM-Assoziation, D-85748 Garching, Germany*
*[6]Laboratorio Nacional de Fusion, Asociacion EURATOM-CIEMAT, Madrid, Spain*
*[7]The national Institute for Laser, Plasma and Radiation Physics, Association EURATOM-MEdC, Magurele-Bucharest, Romania*
*[8]Association "EURATOM - Belgian State" Laboratory for Plasma Physics Koninklijke Militaire School - Ecole Royale Militaire Renaissancelaan 30 Avenue de la Renaissance B-1000 Brussels Belgium*
** See annex of F. Romanelli et al, "Overview of JET Results", (23rd IAEA Fusion Energy Conference, Daejon, Republic of Korea (2010)).*

Preprint of Paper to be submitted for publication in Proceedings of the High Temperature Plasma Diagnostics (HTPD) 2012, Monterey, California, USA.
7th May 2012 - 10th May 2012

**ABSTRACT**

The new JET ITER-like wall (made of beryllium and tungsten) is more fragile than the former Carbon Fiber Composite (CFC) wall and requires active protection to prevent excessive heat loads on the Plasma Facing Components (PFC). Analogue CCD cameras operating in the near infrared wavelength are used to measure surface temperature of the PFCs. Region Of Interest (ROI) analysis is performed in real time and the maximum temperature measured in each ROI is sent to the Vessel Thermal Map (VTM). The protection of the ITER-like wall system started in October 2011 and has already successfully led to a safe landing of the plasma when hot spots were observed on the Be main chamber PFCs. Divertor protection is more of a challenge due to dust deposits that often generate false hot spots. In this contribution we describe the camera, data capture and real time processing systems. We discuss the calibration strategy for the temperature measurements with cross validation with thermal IR cameras and bi-colour pyrometers. Most importantly, we demonstrate that a protection system based on CCD cameras can work and show examples of hot spot detections that stop the plasma pulse. The limits of such a design and the associated constraints on the operations are also presented.

## 1. INTRODUCTION

The new JET ITER-like wall [1], made of beryllium (main chamber), bulk tungsten (outer divertor target) and Carbon Fibre Composite (CFC) coated with tungsten (divertor) is more fragile than its CFC predecessor. The rather low melting point of the beryllium (1257$^{o}$C), the risk of delaminating of the tungsten coating and the temperature threshold at which the bulk tungsten re-crystallises (1200$^{o}$C), require that the Plasma Facing Component (PFC) temperature is constantly monitored in order to avoid overheating and eventual damage of the PFCs. The hot spot detection system relies on imaging diagnostics and bi-colour pyrometers. Imaging systems were already proven to be efficient protection diagnostics on Tore Supra [2] and ASDEX Upgrade [3]. Region Of Interest (ROI) analysis is performed on the video output of 9 CCD cameras in real time and outputs are fed to the Vessel Thermal Map (VTM) [4]. The VTM analyses the temperature data and sends alarms to the real time protection sequencer [5] that will override control systems and reduce the heat loads on the PFCs at risk, by safely landing the plasma, changing the plasma configuration or reducing the additional heating. The Protection of the ITER-like Wall project (PIW) started in February 2010 and commissioning activities started at the beginning of the JET experimental campaigns in October 2011.

## 2. DIAGNOSTIC SYSTEMS

The imaging sensors are analogue monochrome CCD cameras (HITACHI KP/M1AP), equipped with Near InfraRed (NIR) filters. The choice of these cameras was motivated by their excellent reliability in the JET environment. In particular they do not require any magnetic shielding. The inconvenience of this pragmatic choice is the rather low sensitivity around 1μm wavelength (<10%)

and the low dynamic range. We use two types of band pass filters: 980±10nm and 1016±40nm. This is an advantage in terms of optics development (conventional optics can be used) but the risk of suffering from parasitic radiation emitted by the plasma is high. It also makes the detection system more sensitive to dust deposits on the surface of the PFC. The cameras operate in non interlaced mode at 50 fields per second in a binning mode (odd and even lines are exposed together at the same time). The sensor apparent size is 720×288 pixels, with the pixels being twice as high as they are wide, and the exposure time is fixed at 20ms. Where practicable, the light intensity can be controlled by an iris aperture (F/#) in order to adjust the dynamic range.

Given the time constraint on the project, we implemented protection cameras on most of the already existing imaging diagnostics and developed one new wide angle view system with in-vessel optics. Most of the systems are therefore not necessarily optimised for NIR wavelengths. In total two wide angle views, two tangential divertor views (see example in Fig.1) and one top view of the divertor outer target cover 25 to 66% of the first wall and up to 43% of the divertor. The exact coverage depends on the specific PFC. Where possible the number of cameras per field of view was doubled in order to extend the dynamic range. On the top view, the camera systems were complemented with four bicolour pyrometers. The field of view of a pyrometer is a circular spot of about 8mm. They have been aligned in order to cover the key regions of the outer divertor target. One additional pyrometer measures the surface temperature on the inner wall, at the footprint of one nNeutral Beam Injector (NBI). Three other pyrometers are looking at the protection frame surrounding the Lower Hybrid antenna. The advantage of bi-colour pyrometers is that the temperature measurement does not require knowledge of the material emissivity. The total temperature range covered per material is given in Table I. Note that no single camera covers the full temperature range. The temperature range of the pyrometers is 350–1300$^{o}$C. The difference in the temperature range between the materials is mainly due to their different emissivities. The tungsten emissivity is well documented [6], whereas specific research and development activities were necessary to determine the emissivities of the beryllium and of the tungsten coatings. The values of emissivity, $\varepsilon$, that we use are shown in Table I.

A frame grabber converts the analogue output of the CCD camera into a digital, 8 bit, Gigabit Ethernet signal, which is distributed to three different systems by an Ethernet switch: 1) The Real Time Processing Unit (RTPU), 2) The data capture and replay and 3) The live display. The RTPU is a Field Programmable Gate Array (FPGA) board that performs the ROI analysis [7]. Each region of interest outputs 3 signals: the validated maximum temperature and the pixel coordinates, (x,y), corresponding to the position of the hot spot. False hot spots due to neutron hits on the sensor are discarded by using a median filter. The other false hot spots, due for example to dust deposits, are eliminated by using a selection algorithm. This algorithm ignores hot spots that are too small. A dynamic ROI of 5×5 pixels is defined around the hottest pixel. If the minimum number of pixels, $N_{pix}$, above a threshold (in percent of the value of the hottest pixel) is found, the hot spot is considered valid. If not, the next hottest spot is selected and the validation process is repeated. Npix and the

threshold are configurable parameters. For the divertor views, we typically use: $N_{pix} = 5$ and a threshold of 90%. For the wide angle views, where the pixel resolution is lower, we generally use $N_{pix} = 1$ and a threshold of 90%. The image of figure 1 illustrates the tools that are used for image analysis during the commissioning of the system. The PInUP software8 allows us synchronously to replay a selection of movies and visualise the ROI that were loaded in the RTPU as well as the RTPU outputs (temperature and position of the hot spot within the ROI). The direct visualisation of the position of the hot spot within the ROI as well as its temperature value (which is refreshed automatically when scrolling through the frames) has proven to be a very powerful tool for the commissioning of the system.

## 3. COMMISSIONING AND VALIDATION

The protection of the ILW is now running and validation of each individual camera is underway. The response of the protection system to main chamber or divertor hot spots has been commissioned but not necessarily with real temperature outputs. The last step in the commissioning procedure is the validation of the temperature outputs from the RTPU. This is done by cross comparison with another temperature measurement, usually that of a thermal IR camera (typically in the 4μm wavelength) or a bicolour pyrometer9. The scenario in Fig. 2 shows an example of an alarm triggered by a hot spot on the Inner Wall Guard Limiter (IWGL). The plasma was limited on the inner wall. As soon as the temperature measurement remains above the trip level (here 750°C) for longer than the assertion time (here 200ms), an alarm is sent by the VTM and the plasma is moved to the outboard side as illustrated by the change of amplitude of the radial inner and outer gap (RIG and ROG) signals. At the same time the plasma current is safely ramped down. The main chamber temperature measurements were validated by comparison with those of the wide angle thermal IR camera.

Figure 3 shows the temperature outputs of the ROI number 2 (bulk W outer divertor target) of the KL11-P1DA camera (see Fig.1) as a function of comparable measurements taken with a divertor thermal IR camera (KL9B) [6]. The different colours indicate the different phases (ohmic or ELMy H-mode, NBI heated) of different JET pulses (the difference between pulses is mainly the gas fuelling). Up to 800°C, the protection camera overestimates the temperature, especially during the NBI phase. The higher the fuelling rate, the larger the overestimation can be. This is clearly an effect of the parasitic light coming from plasma radiation. Spectroscopy measurements indicate it is due to continuum radiation and that no spectral line is seen by the camera. The effect is less pronounced during the ohmic phase (cooling down after the NBI phase), probably because in that case the absence of ELMs reduces the volumetric emission. Above 800°C, the agreement between the protection camera and the thermal IR camera is within 2.5 % in average. These results were only obtained by imposing a rather large size on the hot spot validation ($N_{pix} = 5$ with a threshold at 90%). This condition allowed us to avoid false hot spots due to dust deposits. These dust particles are not thermally connected to the bulk material and get hot very rapidly but are no danger for the ILW. Their number decreased as conditioning of the divertor progressed but some always remain, especially

close to the edges of the target. The large size of the hot spot imposed as validation condition is justified since, when the bulk tungsten is heated, lateral diffusion will automatically guarantee a minimum size of the hot spot. The same exercise will be repeated for the tungsten coating (e.g. with ROI 4 in Fig.1) as soon as configurations with the strike point on the outer vertical target with high heating power are run. Figure 1 also shows that the inner divertor protection suffers even more from plasma radiation. However, such a high level of plasma radiation is reached here because of the nearly detached conditions, in which in principle the inner divertor target does not overheat. We have not yet seen a scenario with the ILW where the inner divertor target was substantially heated.

## CONCLUSION

The protection system of the JET ITER-like wall has demonstrated its capability of avoiding overheating of the main chamber beryllium wall. The protection of the divertor is more difficult but a sufficient level of protection can be obtained on the outer divertor provided that temperature calibrations are validated, which is ongoing work. The inner divertor measurements suffer more from parasitic light coming from the plasma and an efficient protection has not been demonstrated so far. This is the constraint of having a protection system based on NIR cameras. Furthermore, commissioning is difficult because the validation of the temperature calibration relies on reaching high temperatures of the PFC (typically at least above 800$^{o}$C). Nevertheless, by the end of the 2012 JET experimental campaigns, we plan to have a running system that protects the key plasma facing components.

## ACKNOWLEDGMENTS

This work, supported by the European Communities under the contract of Association between EURATOM and CCFE, was carried out within the framework of the European Fusion Development Agreement. The views and opinions expressed herein do not necessarily reflect those of the European Commission. This work was also part-funded by the RCUK Energy Programme under grant EP/I501045

## REFERENCES

[1]. G.F. Matthews et al., Physica Scripta **T145** (2011) 014001
[2]. P. Moreau et al., Fusion Engineering and Design, **82** 5-14, (2007) p 1030-1035
[3]. A. Herrmann et al., Fusion Engineering and Design, **86** 6-8, (2011) p 530-534
[4]. A. V. Stefen et al., Proceedings of the 13th ICALEPCS, Grenoble (2011)
[5]. D. Alves et al., Proceedings of the 13th ICALEPCS, Grenoble (2011)
[6]. CRC Handbook of Chemistry and Physics, 75th edition, ed. D.R. Lide and H.P.R. Frederikse, CRC Press (1994-95)
[7]. M. Jouve, C. Balorin, D. Kinna, G. Arnoux, P. Carvalho, S. Devaux, P. Thomas, K.-D. Zastrow, J. Veyret and JET-EFDA contributors, Proceedings of the 13th ICALEPCS, Grenoble (2011)

[8]. V. Martin, V. Moncada, G. Dunand, Y. Corre, E. Delchambre and J.M. Travère, Fusion Engineering and Design, **86**, 4-5 (2011) p 270-278

[9]. I. Balboa et al., This conference.

| Material | Emissivity | Temperature range (°C) |
|---|---|---|
| Be | 0.25 | 596 – 1357 |
| $W_{coating}$ | 0.6 | 544 - 2052 |
| W | 0.42 – 1.98*10$^{-5}$*T (K) | 560 - 2248 |

*Table 1: List of temperature ranges covered and emissivities (at 1μm) used for the three materials present in JET: beryllium (Be), tungsten (W) and tungsten coatings (Wcoating) on CFC.*

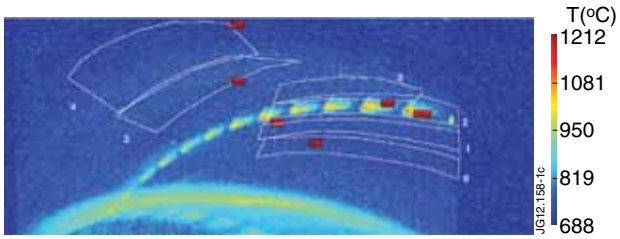


*Figure 1: Image of the divertor view (tangential) taken with the KL11-P1DA camera (JET Pulse No: 82630, frame 1265). The top and bottom of the image show the outer, inner divertor respectively (the view is rotated 90 degrees counterclockwise). At the centre, the hottest areas correspond to the outer strike point. The white areas superimposed correspond to the ROIs (labeled from 0 to 5) used by the RTPU and the red markers indicate the location and temperature of the validated hot spot.*

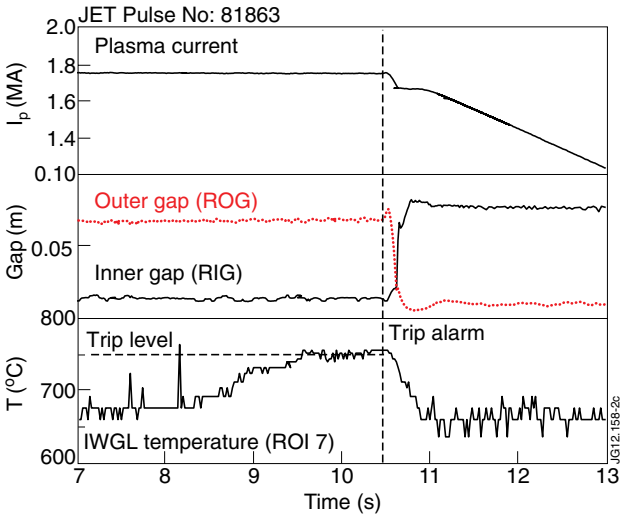


*Figure 2: Evolution of the plasma current, radial outer and inner gaps and temperature output of the RTPU for an ROI monitoring an inner wall guard limiter (IWGL) in a pulse where the trip level is reached and the plasma safely landed.*

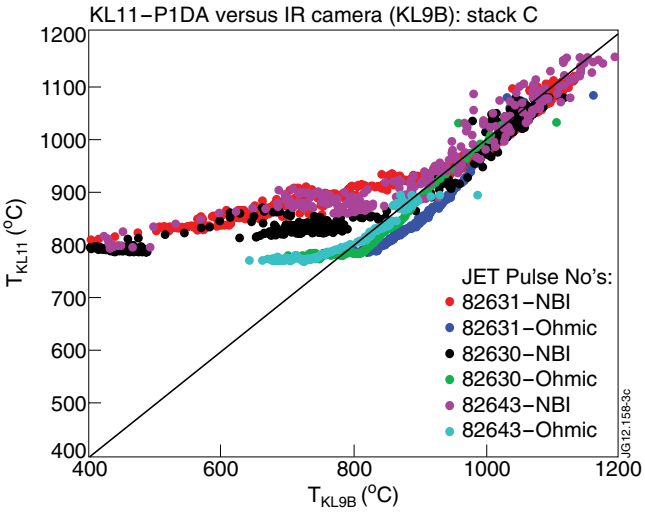


*Figure 3: Real time temperature outputs (ROI #2 of the KL11-P1DA camera) as a function of the temperature measured on a comparable area (stack C of the divertor outer target) by the thermal IR camera (KL9B). Three different plasma pulses, with different fuelling rate are compared. The NBI heating phase is distinguished from the cooling down, ohmic, phase.*